Ultrasonics Sonochemistry 90 (2022) 106210

Contents lists available at ScienceDirect

Ultrasonics Sonochemistry

journal homepage: www.elsevier.com/locate/ultson

# Effects of ultrasound-assisted $H_2O_2$ on the solubilization and antioxidant activity of yeast β-glucan

Xia Ma [a], Lin Dong [a], Yan He [a], Shiwen Chen [b,*]

[a] School of Perfume and Aroma Technology, Shanghai Institute of Technology, No. 100 Haiquan Road, Shanghai 201418, PR China
[b] Shanghai Sixth People's Hospital Affiliated to Shanghai Jiao Tong University School of Medicine, Shanghai 200233, PR China

ARTICLE INFO

*Keywords:*
Ultrasound
$H_2O_2$
Yeast β-glucan
Solubilization
Structure characterization

ABSTRACT

Yeast β-glucan (YG) possess an extensive range of biological activities, such as the inhibition of oxidation, but the poor water solubility of macromolecular YG limits its application. In this study, through the combined degradation of ultrasonic waves and $H_2O_2$, and the optimization of the main process parameters for solubilizing YG by response surface methodology (RSM), a new product of $YG_{UH}$ was generated. The molecular weight, structural characteristics and degradation kinetics before and after solubilization were evaluated. The results showed that the optimal solubilization conditions were reaction time: 4 h, ultrasonic power: 3 W/mL, $H_2O_2$ concentration: 24 %. Under these conditions, ultrasound-assisted $H_2O_2$ increased the solubility (from 13.60 % to 70.00 %) and reduced molecular weight (from $6.73 \times 10^6$ Da to $1.22 \times 10^6$ Da). Fourier transform infrared spectroscopy (FTIR), nuclear magnetic resonance (NMR), Congo red (CR), scanning electron microscopy (SEM) revealed that ultrasound-assisted $H_2O_2$ increased the conformation's flexibility greatly, without changing the main structure of YG. More importantly, solubilization of YG improved free radical scavenging activity with $YG_{UH}$ exhibiting the highest levels of DPPH and $ABTS^+$ free radical scavenging activity. These results revealed that ultrasound-assisted $H_2O_2$ degradation could be a suitable way to increase the solubility of YG for producing value-added YG.

## 1. Introduction

Yeast β-glucan is a natural polysaccharide extracted from yeast cell wall [1], which is composed of a linear backbone of D-glucose connected by β-1,3 bonds and branches of β-1,6 bonds [2], and has higher biological activity than other β-glucans [3]. More and more studies have proved that yeast β-glucan has good biological activities, such as antivirus [4], enhancing immunity [5], anti-cancer [6], lowering cholesterol [7], anti-tumor [8], improve the intestinal flora [9] and other physiological functions. In recent years, yeast β-glucan has been widely used in the functional food, cosmetics and pharmaceutical industries [10,11]. However, the tight triple helix structure and high molecular weight of yeast β-glucan leads to its insolubility, which affects its biological activities and limits its application range. Therefore, it is of great significance to improve the biological activity by using appropriate methods to degrade polysaccharides in order to increase their solubility.

The biological activity of polysaccharides is affected by its molecular weight, structure and conformation [12]. Currently, the commonly used degradation methods of polysaccharides include chemical degradation, physical degradation and biological degradation [13]. Chemically degrading is easy to destroy the original structure and groups of polysaccharides and causes great environmental pollution [14]. The requirement of physical degradation equipment is relatively high [15,16]. The enzymatic degradation method is limited for the enzyme's sensitivity to the surrounding environment and poor stability, furthermore various factors in the solution and the environment can significantly affect the physiology of the enzyme, activity and catalytic reaction rate [17].

Oxidative degradation by $H_2O_2$ has attracted much attention because of its non-toxicity and low cost. The free radical catalyzed $H_2O_2$ method is often used to degrade *Tremella fuciformis* polysaccharide, and the oxidative degradation does not change the main structure of *Tremella fuciformis* polysaccharide with lower molecular weight possessing higher antioxidant activity [18,19]. Wang et al [20] used free radicals to degrade a new glycosaminoglycan in *Holothuria mexicana* (HmG), and found that the degradation rate had a positive correlation with peroxide concentration without destroying the primary structure. Yet, the $H_2O_2$ concentration used in the process determines the rate of degradation to a lower molecular weight. In late research, modified polysaccharides with higher bioactivity could be obtained by combining different degradation

* Corresponding author.
*E-mail addresses:* maxia@sit.edu.cn (X. Ma), 206071107@mail.sit.edu.cn (L. Dong), heyan@sit.edu.cn (Y. He), chenshiwen@126.com (S. Chen).

https://doi.org/10.1016/j.ultsonch.2022.106210
Received 14 September 2022; Received in revised form 11 October 2022; Accepted 21 October 2022
Available online 25 October 2022

methods [21]. Many studies have proved that ultrasonic wave can be used not only as the main means of degradation, but also as an auxiliary condition in oxidative degradation, which can effectively degrading polysaccharides. Ultrasonic wave plays a key role in the oxidative degrade process of $H_2O_2$, and its cavitation effect can accelerate the decomposition of $H_2O_2$ [22]. As far as we know, no other studies have recorded the degradation of YG by ultrasound-assisted $H_2O_2$.

Recently, we studied the ultrasound-assisted enzymatic hydrolysis of YG and demonstrated that increasing the solubility of YG could improve antioxidant activity [23]. On this basis, we have provided an effective method for the preparation of β-glucan with a certain low molecular weight. In this study, we used ultrasound-assisted $H_2O_2$ to solubilize YG, optimized its solubilization conditions by response surface methodology, characterized the structures, and evaluated their antioxidant activity. The purpose of this study was to investigate the effect of ultrasound-assisted $H_2O_2$ degradation on the structure of YG, as well as the degradation kinetic model and its possible mechanism of solubilization of YG.

## 2. Materials and methods

### 2.1. Materials and reagents

The yeast β-glucan content extracted from *Candida utilis* in our laboratory (Shanghai, China) exceeded 82.65 %. Hydrogen peroxide ($H_2O_2$) was purchased from Aladdin Biochemical Technology Co., Ltd., China. All other chemicals and reagents were of analytical reagent grade and were used without further purification.

### 2.2. Preparation of YG

The polysaccharides were extracted from *Candida utilis* using high pressure steam synergistic enzymatic method according to our previous report [24]. The extract was prepared with a 0.02 mol/L pH 7.5 sodium phosphate buffer to prepare a yeast cell suspension with solid–liquid ratio of 10 %, 50 g of glass beads with a diameter of about 0.3 and 0.4 cm were added, and high-pressure steam treatment was performed at 121 °C for 2 h, cooled to room temperature, centrifuged at 8000 rpm for 5 min, and the precipitate was washed twice. Add 2 % neutral protease and papain, adjust to pH 6.0 with 1.0 mol/L sodium hydroxide solution or hydrochloric acid solution, and perform enzymatic hydrolysis for 2 h at 55 °C. The precipitate was prepared into a 1:5 suspension with distilled water, and ultrasonically extracted using the ultrasonic cell crusher JY92-IIDN (Ningbo, Ningbo Xinzhi Biological Technology Co., Ltd., China). Protein was removed by two-phase extraction. The polysaccharide solution was dialyzed for 48 h, and then freeze-dried to obtain YG.

### 2.3. Polysaccharide degradation experiment

#### 2.3.1. Solubility of YG from Candida utilis

The solubility was determined according to the previous method [25]. Briefly, the YG solution was centrifuged at 8000 rpm for 5 min, then the supernatant was put into an aluminum box dried to constant weight, dried at 105 °Cto constant weight, and weighed repeatedly until the mass difference between the two weights did not exceed 2 mg, keeping the final constant weight value. Calculate the solubility according to the following formula.

$$Solubility = W/(C \times V) \quad (1)$$

Where W (g) is the weight of the dried product of the supernatant, C (g/mL) is the initial solution concentration, and V (mL) is the volume of the supernatant.

#### 2.3.2. Response surface optimization experiment

On the basis of single factor experiment, the reaction conditions were optimized by Box-Behnken design (BBD) with three factors and three levels. The Box-Behnken Design (BBD) principle of Design Expert 8.0.5 software was used to design and fit the response surface methodology.

### 2.4. Evaluation of intrinsic viscosity and viscosity-average molecular weight

The intrinsic viscosity [η] of polysaccharides was measured according to the previously reported method [26]. Measured by Ubbelohde viscometer at 25 ± 0.5 °C. The difference in each measurement is<0.2 s, and the average value was taken as the outflow time. From the outflow time, the relative viscosity ($\eta_r$) and the specific viscosity ($\eta_{sp}$) were obtained from the Eqs. (2) and (3). The intrinsic viscosity value [η] can be calculated according to Eqs. (4).

$$\eta_r = t/t_0 \quad (2)$$

$$\eta_{sp} = \eta_r - 1 \quad (3)$$

$$[\eta] = \sqrt{2\eta_{sp} - ln\eta_r}/c \quad (4)$$

Where t and $t_0$ are respectively the flowing times or relative viscosity of the polysaccharide solution and the solvent, $\eta_r$ is the relative viscosity, $\eta_{sp}$ is the incremental viscosity, and c is the concentration of polysaccharide (g/mL).

### 2.5. Fitting of degradation kinetics model

According to the first-order and second-order reaction kinetics, the kinetic model of YG degradation with ultrasound-assisted $H_2O_2$ treatment was evaluated [27]. It is expressed as Eqs. (5) and (6), which are:

$$ln(M_t/M_0) = -kt \quad (5)$$

$$1/M_t - 1/M_0 = kt \quad (6)$$

where $M_0$ and $M_t$ represent the viscosity average molecular weight at the beginning of the reaction and at reaction time, respectively; k is the degradation rate constant ($mol \cdot g^{-1} \cdot min^{-1}$); t is the degradation time (min).

### 2.6. Structure characterization

#### 2.6.1. Molecular weight measurement

The $M_w$ of β-glucan content before and after solubilization was determined by the coupling technique of High performance size exclusion chromatography (HPSEC), and multiangle laser light scattering (MALLS) connected with differential refractive index detector (HPSEC-MALLS-RID, Wyatt, USA). Chromatographic conditions: ShodexOHpak SB HQ 804 and 806 were connected in series, the mobile phase was 0.05 mol/L $NaNO_3$ solution, the flow rate was 0.5 mL/min, the column temperature was 35 ℃, and the injection volume was 100 μL.

#### 2.6.2. Fourier transform infrared spectroscopy (FTIR) analysis

The dried polysaccharide sample was added into agate mortar containing KBr, evenly ground, compressed and scanned by FTIR (Bruker, Germany) at the wavelength range of 4000–500 $cm^{-1}$.

#### 2.6.3. Nuclear magnetic resonance spectroscopy (NMR) analysis

Dissolve 30 mg of β-glucan in 0.6 mL of $d_6$-DMSO at 80 °C. Each β-glucan sample dissolved in $d_6$-DMSO was subjected to $^1H$ and $^{13}C$ NMR analyses.

#### 2.6.4. Congo red test

Congo red solution (80 μmol/L, 1 mL) was mixed with 2 mL of

**Table 1**
Box-Behnken design with independent variables and observed values.

| Runs | Levels of independent factors [a] | | | Solubility (%) |
|---|---|---|---|---|
| | A(h) | B(W/mL) | C (%) | |
| 1 | 4 | 4 | 15 | 57.33 |
| 2 | 3 | 2 | 15 | 51.11 |
| 3 | 4 | 4 | 30 | 63.33 |
| 4 | 3 | 6 | 30 | 59.33 |
| 5 | 3 | 4 | 20 | 64.67 |
| 6 | 3 | 4 | 20 | 65.33 |
| 7 | 4 | 2 | 20 | 64.89 |
| 8 | 2 | 4 | 15 | 45.11 |
| 9 | 3 | 2 | 30 | 58.89 |
| 10 | 3 | 4 | 20 | 64.00 |
| 11 | 3 | 4 | 20 | 65.33 |
| 12 | 3 | 6 | 15 | 48.44 |
| 13 | 4 | 6 | 20 | 61.11 |
| 14 | 2 | 4 | 30 | 61.33 |
| 15 | 2 | 2 | 20 | 43.56 |
| 16 | 3 | 4 | 20 | 66.00 |
| 17 | 2 | 6 | 20 | 67.56 |

[a] A, reaction time (h); B, ultrasonic power (W/mL); C, hydrogen peroxide concentration (%).

**Table 2**
Analysis of variance of regression equation and coefficients.

| Source | Sum of Squares | d f | Mean Square | F-value | p-value | |
|---|---|---|---|---|---|---|
| Model | 859.69 | 9 | 95.52 | 9.541 | 0.003 | significant |
| A-Reaction time | 79.34 | 1 | 79.34 | 7.92 | 0.020 | |
| B-Ultrasonic power | 37.63 | 1 | 37.63 | 3.76 | 0.093 | |
| C-Hydrogen peroxide concentration | 208.99 | 1 | 208.99 | 20.88 | 0.002 | |
| AB | 192.90 | 1 | 192.90 | 19.27 | 0.003 | |
| AC | 25.29 | 1 | 25.29 | 2.53 | 0.155 | |
| BC | 0.094 | 1 | 0.09 | 0.01 | 0.925 | |
| $A^2$ | 12.57 | 1 | 12.57 | 1.25 | 0.299 | |
| $B^2$ | 69.44 | 1 | 69.44 | 6.94 | 0.033 | |
| $C^2$ | 271.72 | 1 | 271.72 | 27.14 | 0.001 | |
| Residual | 70.07 | 7 | 10.01 | | | |
| Lack of fit | 67.76 | 3 | 22.59 | 39.10 | 0.002 | Not significant |
| Pure error | 2.31 | 4 | 0.58 | | | |
| Cor Total | 929.77 | 16 | | | | |

polysaccharide solution. The NaOH solution was added to the mixed solution to 5 mL, and the final concentration of NaOH was 0, 0.05, 0.10–0.50 mol/L, standing for 10 min, and scanning with UV–visible spectrophotometer (UV-2600, Shimadzu, Japan) at 400–600 nm wavelength [28].

#### 2.6.5. Scanning electron microscope (SEM) analysis

β-glucan was coated on a gold disk, and the microstructure of β-glucan was observed and analyzed by scanning electron microscope Hitachi SEM-25009 (Hitachi, Japan) under high vacuum condition with an acceleration voltage of 5 kV and high vacuum condition.

### 2.7. Determination of antioxidant activity in vitro

#### 2.7.1. DPPH radical scavenging activity

The DPPH radical scavenging activity of polysaccharides was studied according to the modified method previously reported [29]. In short, DPPH solution (2 mL 0.2 mmol/L) was added to 2 mL of polysaccharide solutions at different concentrations (0.4-2.0 mg/mL) and mixed evenly. The mixed solutions were reacted in the dark for 30 min with ascorbic acid (VC) as the positive control and anhydrous ethanol as the blank control. The absorbance was measure at 517 nm. Calculate the DPPH radical scavenging activity according to the formula:

$$Scavenging\ activity(\%) = \left[1 - \left(A_i - A_j\right)/A_c\right] \times 100 \quad (7)$$

Where $A_i$ is the absorbance of the sample mixed solution; $A_j$ is the absorbance of the blank group mixed solution; and $A_c$ is the absorbance of the control group mixed solution.

#### 2.7.2. ABTS radical scavenging activity

The scavenging activity of ABTS free radical was determined according to the previous method with some modification [30]. The mixed solution of ABTS solution (7.40 mmol/L) and $K_2S_2O_8$ solution was added to the polysaccharide solutions with different concentrations (0.4-2.0 mg/mL), and mixed evenly. Then reacted in the dark at room temperature for 10 min. The absorbance was measured at 734 nm, and the phosphate buffer was the blank control. The clearance rate was calculated as follows:

$$Scavenging\ activity(\%) = \left[1 - \left(A_i - A_j\right)/A_c\right] \times 100 \quad (8)$$

Where $A_i$ is the absorbance of the sample solution; $A_j$ is the absorbance of the sample solution and phosphate buffer; $A_c$ is the absorbance of the sample-free solution.

### 2.8. Statistical analyses

All experiments were conducted three times, and the data were expressed as means ± standard deviation. Data analysis was performed using Origin 9.0 software (Origin Lab Corporation, Northampton, Mass., USA). One-way analysis of variance (ANOVA) was used to determine the statistical significance, and the value of $P < 0.05$ was considered to be statistically significant.

## 3. Results and discussions

### 3.1. Optimization of ultrasound-assisted $H_2O_2$ solubilization of YG

Generally, time, reaction temperature, $H_2O_2$ concentration, and ultrasonic power significantly affect the solubility of YG. In this study, reaction temperature of 60 °C was set as a fixation factor to determine the optimal conditions for solubilization of YG, as this condition provided the highest solubility by determining the solubility of YG according to a preliminary study (data not shown). Thus, three independent variables, namely time, $H_2O_2$ concentration and ultrasonic power, were established in response surface methodology.

The reaction time (A), ultrasonic power (B) and hydrogen peroxide concentration (C) were selected as three independent variables. An additional 17 BBD experiments were performed to optimize the three independent reaction variables. The BBD matrix and experimental data are shown in Table 1. Using Design Expert 8.0 software to perform regression analysis on the data, the quadratic polynomial regression equation of A, B and C obtained after fitting was: $Y = 67.8 + 3.23A + 2.23B + 5.11C\text{-}6.94AB\text{-}2.45AC\text{-}0.1491BC\text{-}1.73A^2\text{-}4.06B^2\text{-}9.3C^2$.

In Table 2, the F value of the model was 9.54, and the corresponding P value was $< 0.001$, indicating that the model was statistical significance. The F-value and p-value of lack-of-fit were 39.10 and 0.002, respectively, clearly indicating the good fit of the model with the experimental data [31]. The determination coefficient ($R^2$) of the model was 0.9246, which can explain the relationship between response and independent variables. Besides, as shown in Table 2 reaction time (A), ultrasonic power (B) and hydrogen peroxide concentration (C), and the quadratic terms of $B^2$ and $C^2$ revealed an extremely significant effect of YG solubility ($p < 0.001$). Furthermore, at $p < 0.05$, the AB interaction term was positive and significant. The other variables had no influence on the solubility of YG ($p > 0.05$).

The shape of the contour line can intuitively see the magnitude of the interaction effect. The ellipse reflects the significant interaction between

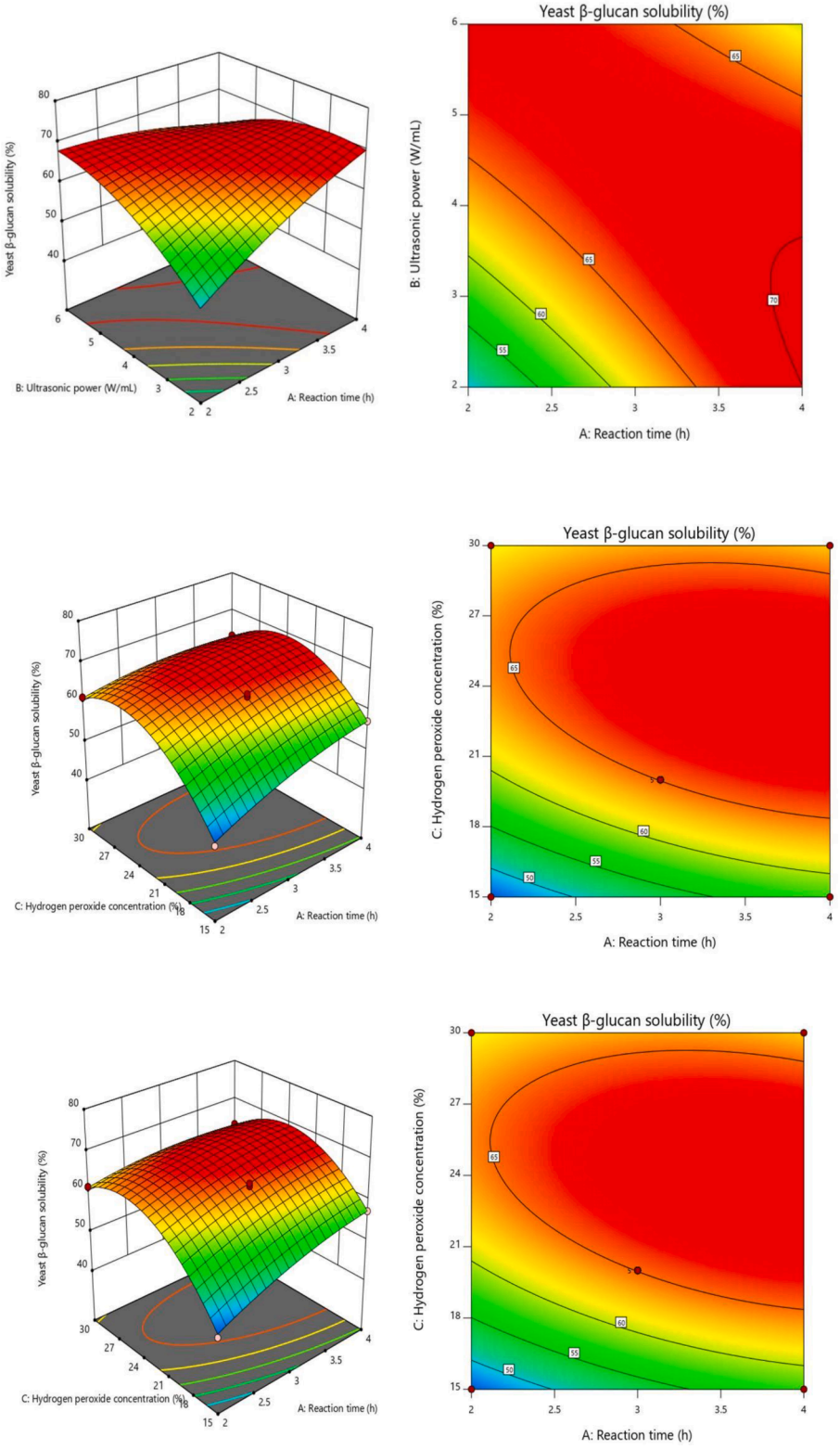


**Fig. 1.** Three-dimensional response surface and two-dimensional contour plots. A reaction time and ultrasonic power, B reaction time and hydrogen peroxide concentration, C ultrasonic power and hydrogen peroxide concentration.

the two factors, and the circular shape is the opposite. The interaction was also significant because the response surface curve is steeper [32]. Only the interaction term of response time and ultrasonic power (AB) was significant, as shown in Fig. 1, which was consistent with Table 2′s findings. The effects of reaction time (A) and ultrasonic power (B), as well as their interactions, on the solubility of the polysaccharide are shown in Fig. 1A. The solubility of the YG increased rapidly with increasing reaction time (A) until 3 h, after which it began to decline. This might be related to the acceleration of molecular motion and response as time passes from 1 h to 3 h. However, after a certain time of reaction, the free radical content no longer increases and the polysaccharide degradation reaction was not significant [33]. The solubility

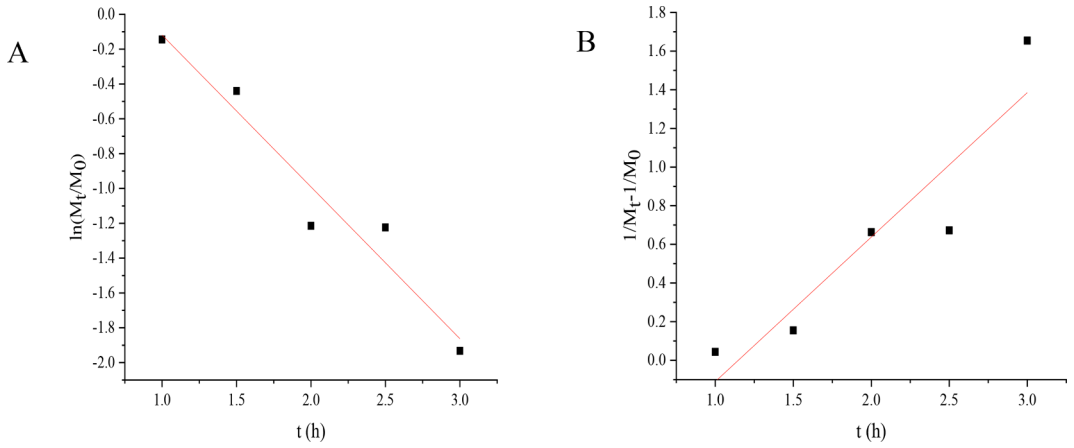


**Fig. 2.** Degradation kinetics curve of YG under ultrasound-assisted $H_2O_2$ treatment A first-order degradation kinetic, B second-order degradation kinetic.

**Table 3**
Degradation kinetic equation and parameters.

| Kinetics | Equation | k | $R^2$ |
|---|---|---|---|
| First-order | ln ($M_t$/3567595.19) = −8.72 t | 8.72 | 0.945 |
| Second-order | 1/$M_t$-1/3567595.19 = 0.7478 t | 0.74 | 0.862 |

of YG rose fast with an increase in hydrogen peroxide concentration until 24 %, then increased marginally, according to Fig. 1B and C. From 15 to 24 %, the hydrogen peroxide concentration exhibited a strong reaction. The solubility then gradually reduced over time. As a consequence, the ANOVA findings indicated that the hydrogen peroxide concentration had the greatest impact on the response value.

According to the solubility measurement, the main effect of ultrasound-assisted $H_2O_2$ on YG was that ultrasonic excitation of $H_2O_2$ produced active radicals. More active radicals such as OH· promoted the degradation of YG. High concentration of $H_2O_2$ was not required for the effective solubilization of YG, because the newly formed hydroxyl radicals might be damaged by excessive $H_2O_2$.

### 3.2. Optimization of degradation condition and its validation

According to the results of the optimization and fitting of the test, the optimal conditions can be obtained: the reaction time was 4 h, the ultrasonic power was 2.80 W/mL, and the hydrogen peroxide concentration was 23.61 %. Adjust according to the actual situation: the reaction time was 4 h, the ultrasonic power was 3 W/mL, and the hydrogen peroxide concentration was 24 %. After model optimization, the solubility of YG reached 70.00 %, indicating that the obtained model has certain practical guiding significance.

Ultrasound-assisted $H_2O_2$ treatment was used to improve the solubility of YG. Ultrasonic wave could promote the oxidative degradation of $H_2O_2$ due to the following two aspects: first, ultrasonic wave could promote the further dissolution of YG and the shearing action caused by the relative motion of solvent molecules and YG molecules would reduce the viscosity of the solution and increase the solubility [34,35]; Second, ultrasonic "cavitation" caused YG to rupture or generate micropores, which promoted the decomposition of $H_2O_2$. The generated ·OH could destroy glycosidic bonds and reduce their molecular weight, thus increasing the solubility [36].

### 3.3. Degradation kinetics model

The kinetic curves and related kinetic parameters of the first- and second-order reactions are shown in Fig. 2 and Table 3 to evaluate the degradation effect of YG by ultrasound-assisted $H_2O_2$ treatment. It was shown that the first-order kinetic model had a higher correlation coefficient ($R^2$) than the second-order kinetic model, which was more suitable for fitting the degradation of YG. The intrinsic viscosity[η] of YG decreased continuously during 2 h of ultrasound-assisted $H_2O_2$ treatment (from 176.54 to 83.59 $cm^3/g$) (Supplementary Table 1). In the

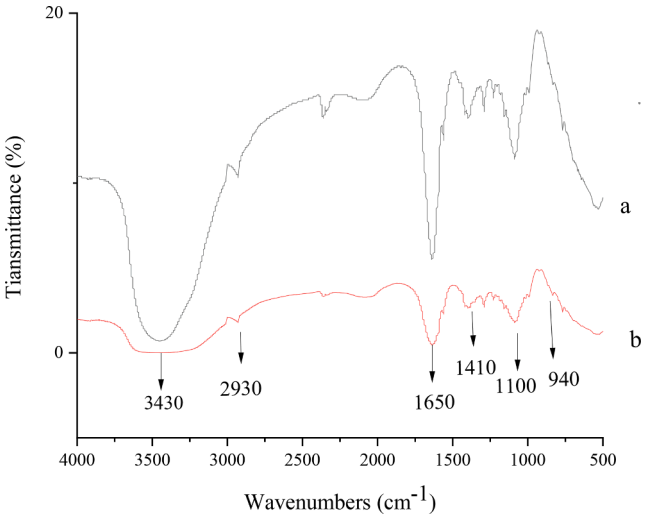


**Fig. 3.** FT-IR spectra of YG (a) and $YG_{UH}$ (b).

**Table 4**
$M_w$, $M_n$, $M_p$, $M_z$ and $M_w/M_n$ of YG and $YG_{UH}$ solubilization.

| β-glucans | $M_w$(×$10^6$Da) | $M_n$(×$10^6$Da) | $M_w/M_n$ | $M_p$(×$10^6$Da) | $M_z$(×$10^6$Da) |
|---|---|---|---|---|---|
| YG | 6.73 ± 1.02 % | 6.55 ± 1.01 % | 1.03 ± 1.43 % | 9.60 ± 1.17 % | 6.93 ± 2.29 % |
| $YG_{UH1}$ | 3.38 ± 1.27 % | 3.23 ± 1.26 % | 1.03 ± 1.43 % | 5.33 ± 1.13 % | 3.56 ± 2.84 % |
| $YG_{UH2}$ | 3.19 ± 1.42 % | 2.90 ± 1.45 % | 1.10 ± 2.04 % | 4.05 ± 1.28 % | 3.545 ± 3.15 % |
| $YG_{UH3}$ | 2.04 ± 1.68 % | 1.83 ± 1.80 % | 1.12 ± 2.46 % | 2.95 ± 1.58 % | 2.29 ± 3.67 % |
| $YG_{UH4}$ | 1.91 ± 1.68 % | 1.72 ± 1.79 % | 1.11 ± 2.45 % | 2.19 ± 1.60 % | 2.14 ± 3.66 % |
| $YG_{UH5}$ | 1.22 ± 2.56 % | 1.09 ± 3.13 % | 1.12 ± 4.04 % | 1.64 ± 1.89 % | 1.37 ± 5.30 % |

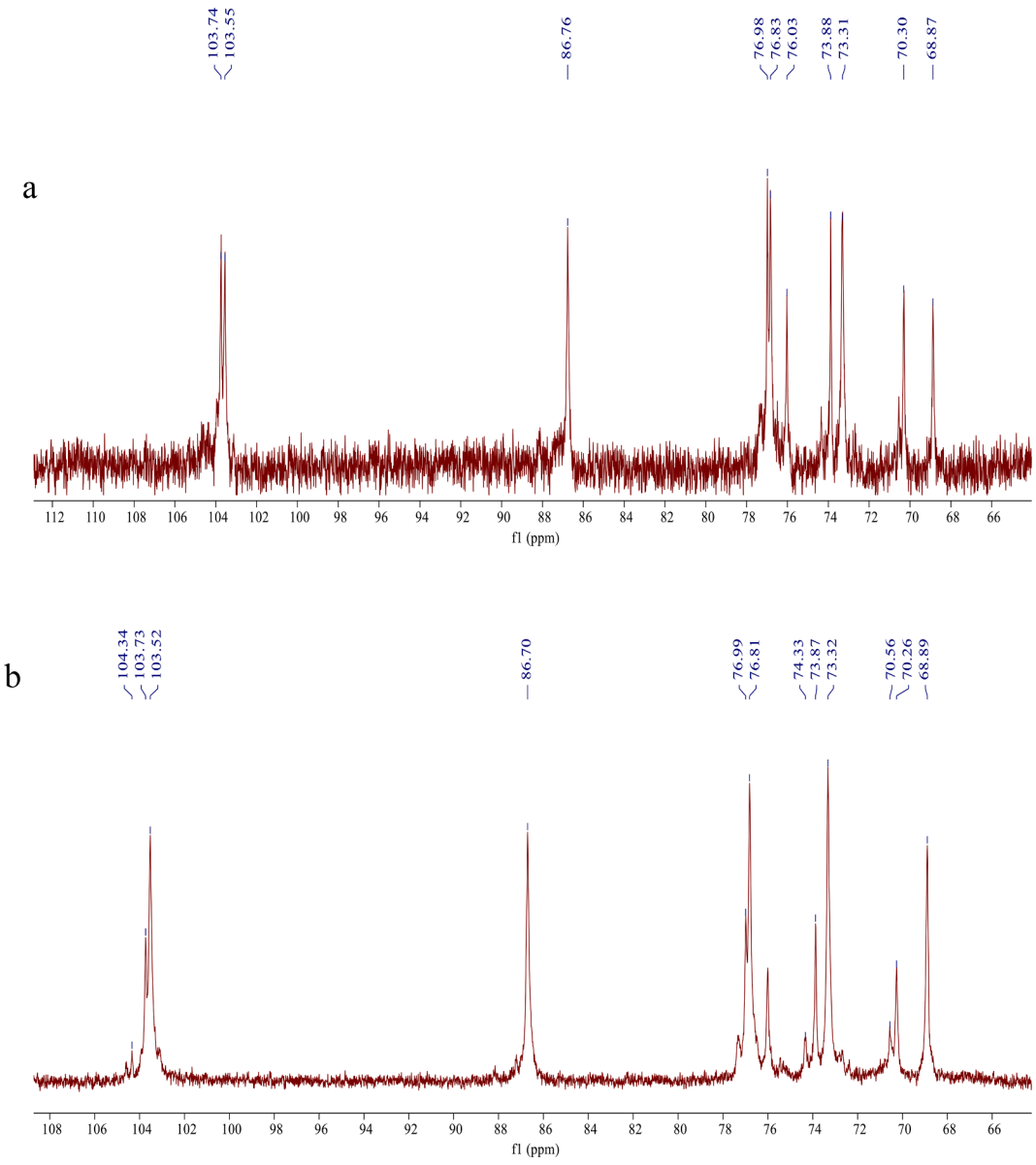


**Fig. 4.** $^{13}C$ NMR spectra of YG (a) and $YG_{UH}$ (b).

early stage of treatment, the intrinsic viscosity dropped sharply to a very low level, and the decrease in intrinsic viscosity was equivalent to the decrease in the average relative molecular mass. Therefore, it can be considered that the ultrasound-assisted $H_2O_2$ method led to the degradation of YG. The reduction in viscosity is not only related to polymer degradation (polymer chain scission or glycosidic bond scission), but also to polymer breakdown. The above results indicated that ultrasound-assisted $H_2O_2$ treatment of polysaccharides was helpful to break the glycosidic bonds, resulting in the decrease of $M_\eta$ and the formation of some small molecular polysaccharides [37]. The production of OH· was related to the content of $H_2O_2$ [38], ultrasonic could promote $H_2O_2$ to generate free radicals (OH·), and then OH· attacked the H atom of the C bond, leading to the formation of carbon-centered free radicals in polysaccharides. A series of free radical reactions occurred in polysaccharides, leading to the breakage of glycosidic bonds and increasing the solubility of YG. Free radicals were slowly produced and gradually disappeared with the decrease of $H_2O_2$ content in the late stage, so $M_\eta$ almost remained unchanged.

### 3.4. Molecular weight

As the degradation time increased, the molecular weight of YG decreased from $6.73 \times 10^6$ Da to $1.22 \times 10^6$ Da. The molecular weights of a series of degraded polysaccharides are shown in Table 4. The molecular weight of YG decreases with time in all β-glucan samples. By controlling the reaction conditions, YG with molecular weights ranging from $1.22 \times 10^6$ Da to $3.38 \times 10^6$ Da can be prepared. Therefore, by selecting reaction conditions, yeast β-glucans of a specific molecular weight range can be prepared [39]. The decrease of molecular weight confirmed that ultrasound-assisted $H_2O_2$ could degrade YG. The bubble collapse caused by ultrasonic induced cavitation generated shear force and formed shock wave, which promoted the decomposition of ·OH by $H_2O_2$ and led to the destruction of intramolecular and intermolecular bonds in YG, cutting the glycosidic bond of YG, leading to the reduction of its molecular weight.

### 3.5. Fourier transform infrared spectroscopy

The spectra of YG (a), $YG_{UH}$ (b) are shown in Fig. 3 in the range of

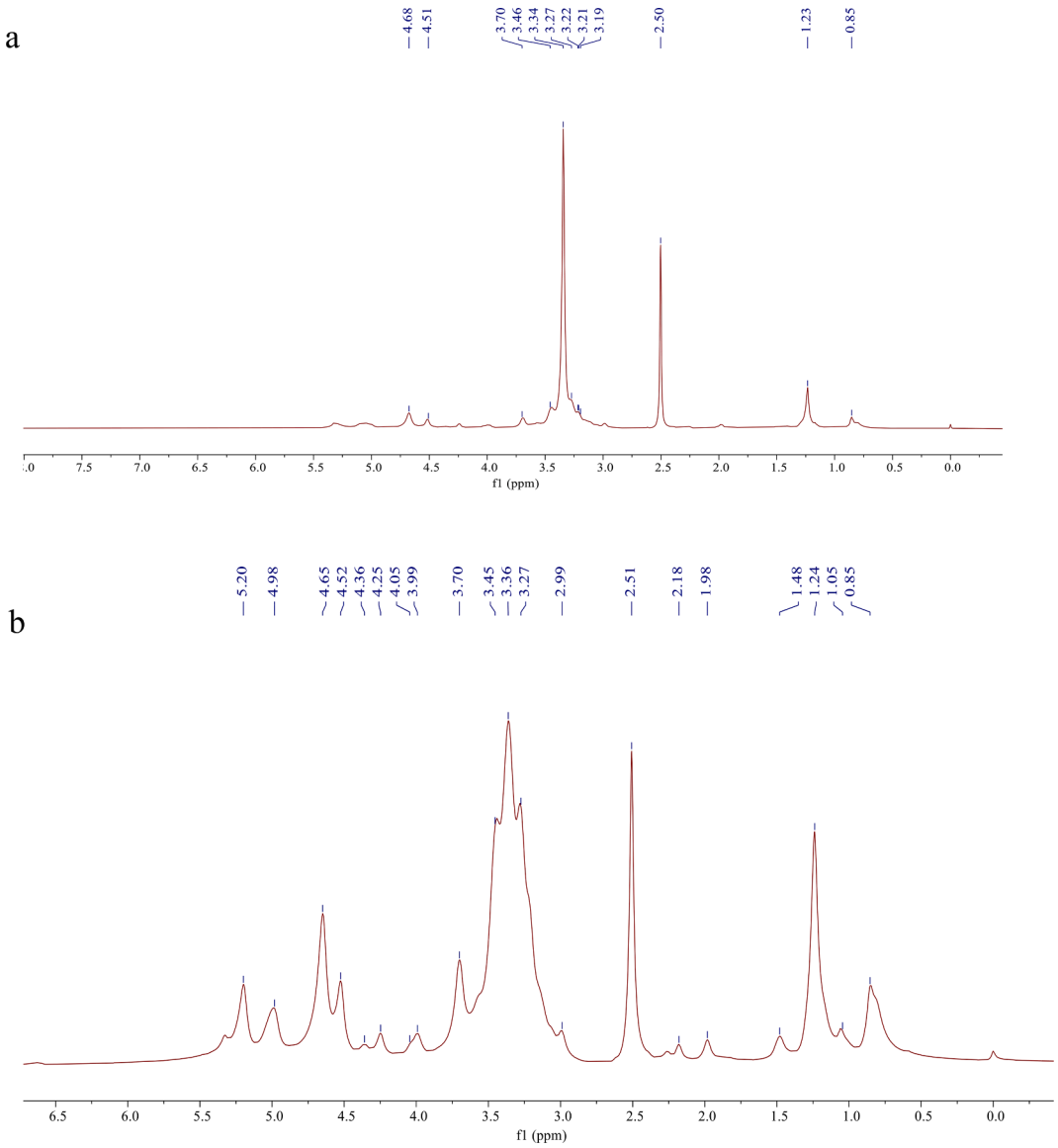


**Fig. 5.** $^{1}$H NMR spectrum of YG (a) and $YG_{UH}$ (b).

4000–500 $cm^{-1}$. The FT-IR spectra of YG and $YG_{UH}$ were not significantly different. 3430 $cm^{-1}$ was the stretching vibration peak of OH in sugar compound C-OH [40], the absorption peak near 1650 $cm^{-1}$ was the C═O asymmetric tensile vibration in —CHO, and the absorption peak in the range of 1400–1200 $cm^{-1}$ further indicated that the sample was a carbohydrate [41]. The characteristic peak near 2930 $cm^{-1}$ was the characteristic absorption peak of C—H on saturated carbon [42]. The absorption peak at 1380 $cm^{-1}$ can indicate that the YG was still connected by β-1,3 bonds after degradation [43]. The two polysaccharides had similar characteristic absorption peaks in the range of 4000–500 $cm^{-1}$, indicating that ultrasound-assisted $H_2O_2$ degradation of YG did not affect the main functional groups of polysaccharides.

### 3.6. Nuclear magnetic resonance spectroscopy

The chemical structures of YG before and after solubilization were preliminarily identified by $^{1}$H- and $^{13}$C NMR. The $^{13}$C NMR spectrum of YG and $YG_{UH}$ are shown in Fig. 4. As shown in the Fig. 4a, YG had six strong signal peaks at $\delta$ 103.55, 73.31, 76.83, 86.76, 70.30 and 68.87 ppm, respectively, which were attributed to the C-1, C-2, C-3, C-4, C-5 and C-6 formants on the β-glucan ring, consistent with the structure of YG in the previously reported [44], indicating that YG was a macromolecular polysaccharide connected by β-(1–3) glycosidic bond [45]. Several weak signal peaks at $\delta$ 69–70 ppm, $\delta$ 73–76 ppm, indicating that there were β-(1–6) glycosidic-linked branches in the YG molecule, but due to the weaker signal peaks, the number of branches was low [46]. In Fig. 4b, the six strong signal peaks at $\delta$ 103.52, 73.32, 76.81, 86.70, 70.26 and 68.89 ppm of the $YG_{UH}$ can be assigned to C-1, C-2, C-3, C-4, C-5 and C-6 [47], indicating that the solubilization of YG by ultrasound-assisted $H_2O_2$ method did not damage its main chain structure, and it was still a glucan molecule linked by β-(1–3) glycosidic bonds [48]. Different from the infrared spectrum of YG, $YG_{UH}$ showed new signal peaks at $\delta$ 74.33 ppm, 76.99 ppm and 103.73 ppm, indicating that a carbon position in the sugar molecule has been replaced. Therefore, the basic skeleton of the modified and solubilized YG was not changed, and the ultrasound-assisted $H_2O_2$ solubilization of YG might act on the 1,6-glycosidic bond in the side chain.

In the $^{1}$H NMR spectrum, the α- or β-configuration of the glycosidic bond is mainly determined by the proton peak on the anomeric C-1. If the chemical shift of the anomeric proton is $\delta$ 4.00–5.00 ppm, it is generally considered to be the β-type. Conversely, if the chemical shift $\delta$ 5.00–6.00 ppm, it is considered to be α type [49]. According to Fig. 5a,

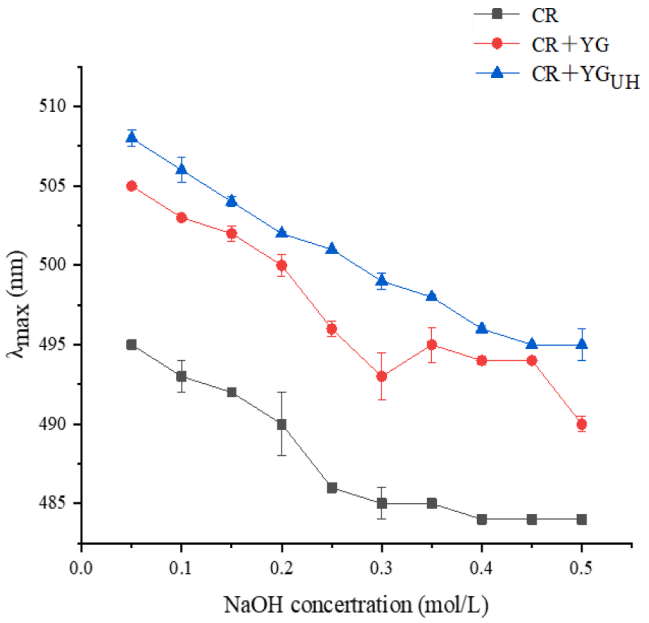


**Fig. 6.** Maximum absorption ($\lambda_{max}$) of Congo red and Congo red + polysaccharose at various NaOH concentrations. (For interpretation of the references to colour in this figure legend, the reader is referred to the web version of this article.)

2.50 ppm was the signal peak of DMSO, the H-1 chemical shift of YG was $\delta$ 4.51 ppm, and it can be seen that most of the chemical shifts of all the anomeric protons were in the range of 3.00–5.00 ppm, which was a typical polysaccharide absorption peak signal [50]. The chemical shift at $\delta$ 3.34 ppm represents H-2, 4, and 5 of the 1,3-linked β-D-Glcp. In addition, the chemical shift of yeast β -glucan at $\delta$ 3.70 ppm was the proton signal of H-6. As shown in Fig. 5b, H-4 and H-5 protons of YG show slight high-field shift, and it was possible that the combination of hydroxyl radical and hydrogen atom destroys the pre-existing intramolecular and intermolecular hydrogen bonds of β-glucan and thus increases its solubility.

### 3.7. Congo red

Congo red is an acid dye which can combine with triple helix polysaccharide in a certain concentration of NaOH solution, and the maximum absorption wavelength ($\lambda_{max}$) of Congo red-polysaccharide complex is red-shifted [51]. In Fig. 6, the red shift of the Congo red-polysaccharide complex formed by the polysaccharide sample and Congo red solution in 0.05–0.50 mol/L NaOH was observed. With the increase of NaOH concentration, the maximum absorption wavelength of Congo red-polysaccharide complex was gradually decreased, indicating that YG and $YG_{UH}$ had triple helix structure. The stability of the triple helical structure of polysaccharides in solution mainly depends on intramolecular and intermolecular hydrogen bonds. The breaking of hydrogen bonds will destroy the triple helix structure [52]. The triple helix structure of YG was not damaged by ultrasound-assisted $H_2O_2$ degradation.

### 3.8. Scanning electron microscope observation

As shown in Fig. 7, the morphology and structure of YG were significantly different before and after solubilization. Before treatment, YG existed in the form of compact aggregated clusters with rough surface and honeycomb-like structure. Fig. 7b was a SEM image of YG after degradation, which was looser and has smaller fragments than YG before treatment. The results suggested that ultrasound-assisted $H_2O_2$ degradation could hinder the aggregation of YG macromolecules and lead to microstructural changes. This might be due to the generation of more hydroxyl radicals by ultrasound-assisted $H_2O_2$, which led to the breakage of YG glycosidic bond, and the decrease of molecular weight also confirmed this.

### 3.9. In vitro antioxidant activities of YG

The in vitro antioxidant activity of YG before and after solubilization was studied by determining the DPPH radical and $ABTS^+$ radical scavenging activity (Fig. 8). As shown in Fig. 8a, with the increase of polysaccharide concentration, the scavenging rate of YG and $YG_{UH}$ on DPPH free radical showed an upward trend. At the polysaccharide concentration of 3.0 mg/mL, the DPPH radical scavenging activities of YG and $YG_{UH}$ were 58.50 % and 80.10 %, respectively. At 3.0 mg/mL, the DPPH radical scavenging rate of $V_C$ reached 95.67 %, and the scavenging rate remained basically unchanged with the increase of concentration. Within the concentration range of 0.4–2.0 mg/mL, the DPPH scavenging activity of $YG_{UH}$ solubilized by ultrasound-assisted $H_2O_2$ method was significantly higher than that of YG. This might be due to the degradation of YG by ultrasound-assisted $H_2O_2$, resulting in the decrease of the molecular weight of YG, and more hydroxyl groups exposed to the solution, thus providing more hydrogen or electrons [53].

As shown in Fig. 8b, the removal efficiency of $ABTS^+$ by the solubilized yeast β -glucan was significantly better than that of the original YG. The results showed that the removal efficiency was enhanced with the increase of polysaccharide concentration. At a polysaccharide concentration of 2.0 mg/mL, the clearance of $ABTS^+$ by YG and $YG_{UH}$ was 34.40 % and 44.00 %, respectively. At 1.2 mg/mL, the $ABTS^+$ radical

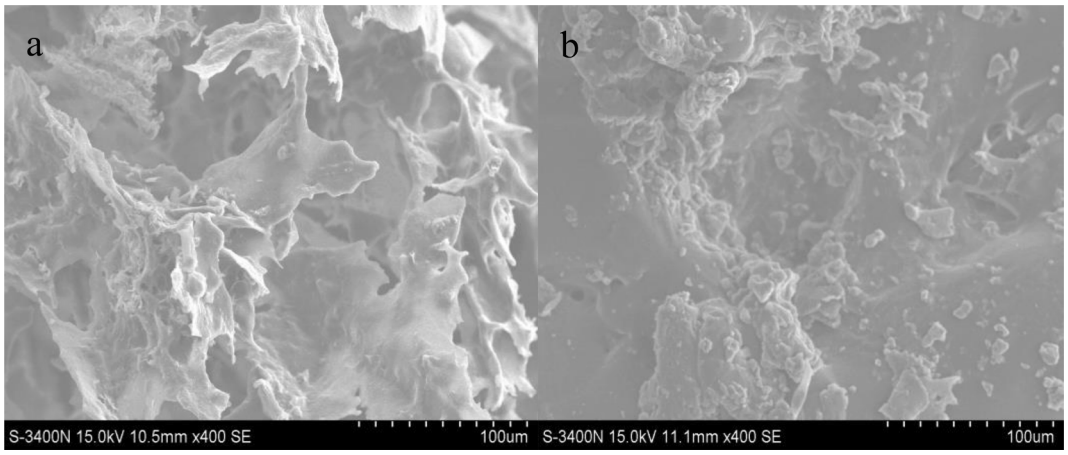


**Fig. 7.** SEM images of YG (a) and $YG_{UH}$ (b) (magnification 400×, Scale bar 100 μm).

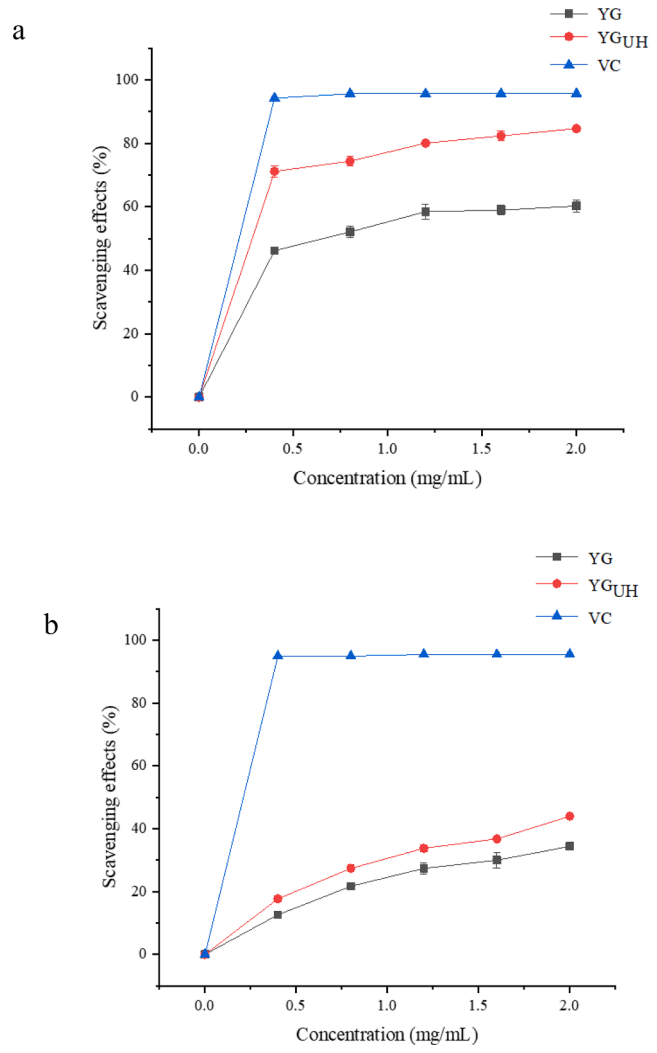


**Fig. 8.** Free radical scavenging activities of YG and $YG_{UH}$ including (a) DPPH scavenging rate, and (b) $ABTS^{+}$ scavenging rate.

scavenging activity of $V_C$ was 95.50 %, and there was no significant change after that. It was possible that low molecular weight polysaccharides contain more free hydroxyl groups, which might be beneficial to improve their antioxidant activity. The antioxidant activity of $YG_{UH}$ in vitro was higher than that of YG, which may be due to the better water solubility of degraded YG, so it was easier to contact free radicals.

## 4. Conclusion

In this study, it was discovered that ultrasound-assisted $H_2O_2$ treatment was a simple and effective method to increase YG solubility and reduce molecular weight. When the ultrasonic intensity was 3 W/mL, the reaction time was 4 h, and the hydrogen peroxide concentration was 24 %, the solubility of YG reached a maximum value. The effect of ultrasound-assisted $H_2O_2$ degradation of YG conformed to the first-order kinetic model, which can believe that ultrasound-assisted $H_2O_2$ can cause degradation of YG. During the degradation of YG, ultrasonic accelerated the decomposition of $H_2O_2$, which resulted in the breakage of YG glycosidic bonds, hindered the aggregation of macromolecules, reduced the molecular weight and improved the solubility, but the primary structure did not change obviously. The antioxidant activity of YG was significantly increased after solubilization. In summary, this study provided an effective method to increase the solubility of yeast β-glucan which would further contribute to the development and utilization of the biological function of yeast β-glucan.

## CRediT authorship contribution statement

**Xia Ma:** Conceptualization, Formal analysis, Supervision, Writing – review & editing. **Lin Dong:** Conceptualization, Data curation, Formal analysis, Writing – review & editing. **Yan He:** Investigation, Methodology, Software, Visualization, Writing – original draft. **Shiwen Chen:** Investigation, Methodology, Software, Visualization, Writing – original draft.

## Declaration of Competing Interest

The authors declare that they have no known competing financial interests or personal relationships that could have appeared to influence the work reported in this paper.

## Data availability

The authors are unable or have chosen not to specify which data has been used.

## Acknowledgements

This work was financially supported by the Shanghai Science and Technology Commission (21142202800); the Collaborative Innovation Fund Project of Shanghai Institute of Technology (xtcx2022-17).

## Appendix A. Supplementary data

Supplementary data to this article can be found online at https://doi.org/10.1016/j.ultsonch.2022.106210.

## References

[1] X. Mo, Y. Sun, X. Liang, L. Li, S. Hu, Z. Xu, S. Liu, Y. Zhang, X. Li, L. Liu, Insoluble yeast β-glucan attenuates high-fat diet-induced obesity by regulating gut microbiota and its metabolites, Carbohyd. Polym. 281 (2022), 119046.
[2] Y. Zhang, D. Wang, Y. Chen, T. Liu, S. Zhang, H. Fan, H. Liu, Y. Li, Healthy function and high valued utilization of edible fungi, Food Sci. Hum. Well. 10 (04) (2021) 408–420.
[3] A. Boutros, A.S. Jean, Magee, Donald Cox, Comparison of structural differences between yeast β-glucan sourced from different strains of *saccharomyces cerevisiae* and processed using proprietary manufacturing processes, Food Chem. 367 (2022), 130708.
[4] P.T. Seven, S.I. Mutlu, I. Seven, G. Arkali, S.O. Kaya, O.E. Kanmaz, Protective role of yeast beta-glucan on lead acetate-induced hepatic and reproductive toxicity in rats, Environ. Sci. Pollut. Res. 28 (38) (2021) 53668–53678.
[5] J.S. Chae, H. Shin, Y. Song, H. Kang, C.H. Yeom, S. Lee, Y.S. Choi, Yeast (1→3)-(1→6)-β-d-glucan alleviates immunosuppression in gemcitabine-treated mice, Int. J. Biol. Macromol. 136 (2019) 1169–1175.
[6] P. de Graaff, C. Berrevoets, C. Rösch, H.A. Schols, K. Verhoef, H.J. Wichers, R. Debets, C. Govers, Curdlan, zymosan and a yeast-derived β-glucan reshape tumor-associated macrophages into producers of inflammatory chemo-attractants, Cancer Immunol. Immun. 70 (2) (2021) 547–561.
[7] R. Kaur, M. Sharma, D. Ji, M. Xu, D. Agyei, Structural features, modification, and functionalities of beta-glucan, J. Nat. Fibers 8 (1) (2019) 1.
[8] N. Wang, H. Liu, G. Liu, M. Li, X. He, C. Yin, H. Yin, Yeast β-D-glucan exerts antitumour activity in liver cancer through impairing autophagy and lysosomal function, promoting reactive oxygen species production and apoptosis, Redox Biol. 32 (2020), 101495.
[9] Y.Y. Cui, X.Y. Ma, Biological function of zymosan and its effect on intestinal health of piglets, J. Anim. Physiol. An. N. 30 (3) (2018) 857–864.
[10] C. Carballo, P.I. Pinto, A.P. Mateus, C. Berbel, C.C. Guerreiro, J.F. Martinez-Blanch, F.M. Codoñer, L. Mantecon, D.M. Power, M. Manchado, Yeast β-glucans and microalgal extracts modulate the immune response and gut microbiome in Senegalese sole (*Solea senegalensis*), Fish Shellfish Immunol. 92 (2019) 31–39.
[11] W. Fu, G. Zhao, J. Liu, Effect of preparation methods on physiochemical and functional properties of yeast β-glucan, LWT-Food Sci, Technol. 160 (2022) 113284.
[12] P. Li, C. Xiong, W. Huang, Gamma-irradiation-induced degradation of the water-soluble polysaccharide from *Auricularia polytricha* and its anti-hypercholesterolemic activity, Molecules 27 (2022) 1110.

[13] F. Xiong, X. Li, L. Zheng, N. Hu, M. Cui, H. Li, Characterization and antioxidant activities of polysaccharides from *Passiflora edulis* Sims peel under different degradation methods, Carbohyd. Polym. 218 (2019) 46–52.
[14] Y. Ishimoto, K.-I. Ishibashi, D. Yamanaka, Y. Adachi, K. Kanzaki, Y. Iwakura, N. Ohno, Production of low-molecular weight soluble yeast β-glucan by an acid degradation method, Int. J. Biol. Macromol. 107 (2018) 2269–2278.
[15] J.K. Yan, Y.Y. Wang, H.L. Ma, Z.B. Wang, Ultrasonic effects on the degradation kinetics, preliminary characterization and antioxidant activities of polysaccharides from *Phellinus linteus* mycelia, Ultrason. Sonochem. 29 (2016) 251–257.
[16] N.T. Long, N.T.N. Anh, B.L. Giang, H.N. Son, L.Q. Luan, Radiation degradation of β-glucan with a potential for reduction of lipids and glucose in the blood of mice, Polymers-Basel. 11 (6) (2019) 955.
[17] J. Wu, P. Li, D. Tao, H. Zhao, R. Sun, F. Ma, B. Zhang, Effect of solution plasma process with hydrogen peroxide on the degradation and antioxidant activity of polysaccharide from *Auricularia auricula*, Int. J. Biol. Macromol. 117 (2018) 1299–1304.
[18] Z. Zhang, X. Wang, M. Zhao, H. Qi, Free-radical degradation by Fe2+/Vc/H2O2 and antioxidant activity of polysaccharide from *Tremella fuciformis*, Carbohyd. Polym. 112 (2014) 578–582.
[19] H. Yuan, L. Dong, Z. Zhang, Y. He, X. Ma, Production, structure, and bioactivity of polysaccharide isolated from *Tremella fuciformis*, Food Sci. Hum. Well. 11 (4) (2022) 1010–1017.
[20] J. Mou, C. Wang, Q. Li, X.H. Qi, J. Yang, Preparation and antioxidant properties of low molecular holothurian glycosaminoglycans by H2O2/ascorbic acid degradation, Int. J. Biol. Macromol. 107 (2018) 1339–1347.
[21] O.S. Ayanda, S.M. Nelana, E.B. Naidoo, Ultrasonic degradation of aqueous phenolsulfonphthalein (PSP) in the presence of nano-Fe/H2O2, Ultrason. Sonochem. 47 (2018) 29–35.
[22] W. Hu, S. Chen, D. Wu, J. Zheng, X. Ye, Ultrasonic-assisted citrus pectin modification in the bicarbonate-activated hydrogen peroxide system: Chemical and microstructural analysis, Ultrason. Sonochem. 58 (2019) 104576.
[23] H. Yuan, Y. He, H. Zhang, X. Ma, Ultrasound-assisted enzymatic hydrolysis of yeast β-glucan catalyzed by β-glucanase: Chemical and microstructural analysis, Ultrason. Sonochem. 86 (2022) 106012.
[24] X. Ma, L.T. Liu, L. Shen, Effects of extraction methods on the properties of *Candida utilis* β-glucan, Food Sci. 39 (11) (2018) 119–125.
[25] H. Liu, W. Bai, L. He, X. Li, Q. Wang, Degradation mechanism of *Saccharomyces cerevisiae* β-D-glucan by ionic liquid and dynamic high pressure microfluidization, Carbohyd. Polym. 241 (2020) 116123.
[26] Y. Diao, M. Song, Y. Zhang, L.Y. Shi, Y. Lv, R. Ran, Enzymic degradation of hydroxyethyl cellulose and analysis of the substitution pattern along the polysaccharide chain, Carbohyd. Polym. 169 (2017) 92.
[27] H. Yang, J. Bai, C. Ma, L. Wang, X. Li, Y.u. Zhang, Y. Xu, Y.u. Yang, Degradation models, structure, rheological properties and protective effects on erythrocyte hemolysis of the polysaccharides from *Ribes nigrum L*, Int. J. Biol. Macromol. 165 (2020) 738–746.
[28] Y. Xu, X. Niu, N. Liu, Y. Gao, L. Wang, G. Xu, X. Li, Y.u. Yang, Characterization, antioxidant and hypoglycemic activities of degraded polysaccharides from blackcurrant (*Ribes nigrum L.*) fruits, Food Chem. 243 (2018) 26–35.
[29] M.J. Shi, X. Wei, J. Xu, B.J. Chen, D.Y. Zhao, S. Cui, T. Zhou, Carboxymethylated degraded polysaccharides from *Enteromorpha prolifera*: Preparation and in vitro antioxidant activity, Food Chem. 215 (2017) 76–83.
[30] S. Zhang, X.Z. Li, Z.P. Wu, C.T. Kuang, Antioxidant activity of polysaccharide from camellia cake against abts and dpph free radicals, Adv. Mater. Res. 550–553 (2012) 1545–1549.
[31] L.Y. Xie, T. Wei, Y. Guo, D.H. Jia, W.H. Peng, B.C. Gan, Application of Response Surface Methodology for Optimization of Liquid Fermentation Medium for Intracellular Polysaccharide Production by *Phellinus baumii*, Food Sci. 31 (7) (2011) 224–228.
[32] J. Prakash Maran, S. Manikandan, K. Thirugnanasambandham, C. Vigna Nivetha, R. Dinesh, Box-Behnken design based statistical modeling for ultrasound-assisted extraction of corn silk polysaccharide, Carbohy. Polym. 92 (1) (2013) 604–611.
[33] X. Chen, D. Sun-Waterhouse, W. Yao, X. Li, M. Zhao, L. You, Free radical-mediated degradation of polysaccharides: Mechanism of free radical formation and degradation, influence factors and product properties, Food Chem. 365 (2021) 130524.
[34] H. Jiang, L.M. Kong, C. Wang, Optimization of degradation conditions and biological activity of polysaccharides from porphyra, Food Sci. 42 (03) (2021) 38–47.
[35] Y. Ren, Z. Wu, M. Shen, L. Rong, J. Xie, Improve properties of sweet potato starch film using dual effects: Combination *Mesona chinensis* Benth polysaccharide and sodium carbonate, LWT- Food Sc. Technol. 140 (2021) 110679.
[36] F. Ma, J. Wu, P. Li, D. Tao, H. Zhao, B. Zhang, L. Bin, Effect of solution plasma process with hydrogen peroxide on the degradation of water-soluble polysaccharide from *Auricularia auricula*. II: Solution conformation and antioxidant activities in vitro, Carbohyd Polym. 198 (2018) 575–580.
[37] Y.J. Gao, H.T. Lv, Research on degradation of polysaccharides from *Promena prolifera* and its scavenging activity of hydroxyl radicals by acid method, Food Sci. 34 (16) (2013) 62–66.
[38] X. Chen, R. Zhang, Y. Li, X. Li, K. Hileuskaya, Degradation of polysaccharides from *Sargassum fusiforme* using UV/H2O2 and its effects on structural characteristics, Carbohyd. Polym. 230 (2020) 115647.
[39] S. Zha, Q. Zhao, B. Zhao, J. Ouyang, J. Mo, J. Chen, L. Chao, H. Zhang, Molecular weight controllable degradation of *Laminaria japonica* polysaccharides and its antioxidant properties, J. Ocean Univ. China 15 (2016) 637–642.
[40] A.A. Khan, A. Gani, F.A. Masoodi, F. Amin, I.A. Wani, F.A. Khanday, A. Gani, Structural, thermal, functional, antioxidant & antimicrobial properties of β-d-glucan extracted from baker's yeast (*Saccharomyces cereviseae*)-Effect of γ-irradiation, Carbohyd. Polym. (2016) 442–450.
[41] A. Xu, G. Xin, Y.B. Zhang, Z. Li, J. Wang, Efficient and sustainable solvents for lignin dissolution: Aqueous choline carboxylate solutions, Green Chem. 19 (17) (2017) 4067–4073.
[42] Y. Cao, S. Zou, H. Xu, M. Li, Z. Tong, M. Xu, X. Xu, Hypoglycemic activity of the Baker's yeast β-glucan in obese/type 2 diabetic mice and the underlying mechanism, Mol. Nutr. Food Res. 60 (12) (2016) 2678–2690.
[43] H. Liu, Y. Li, J. Gao, A. Shi, L.i. Liu, H. Hu, N. Putri, H. Yu, W. Fan, Q. Wang, Effects of microfluidization with ionic liquids on the solubilization and structure of β-d-glucan, Int. J. Biol. Macromol. 84 (2016) 394–401.
[44] S. Freimund, M. Sauter, H. Othmar Kppeli, Dutler,, A new non-degrading isolation process for 1,3-β-d-glucan of high purity from baker's yeast *Saccharomyces cerevisiae*, Carbohyd. Polym. 54 (2003) 159–171.
[45] D.L. Williams, R.B. McNamee, E.L. Jones, H.A. Pretus, H.E. Ensley, I.W. Browder, N.R. Di Luzio, A method for the solubilization of a (1→3)-β-D-glucan isolated from *Saccharomyces cerevisiae*, Carbohyd. Res. 219 (1991) 203–213.
[46] Y. Wang, Y. Liu, H. Yu, S. Zhou, Z. Zhang, D. Wu, M. Yan, Q. Tang, J. Zhang, Structural characterization and immuno-enhancing activity of a highly branched water-soluble β-glucan from the spores of *Ganoderma lucidum*, Carbohyd. Polym. 167 (2017) 337–344.
[47] L.Q. Luan, N. Uyen, Radiation degradation of (1→3)-β-D-glucan from yeast with a potential application as a plant growth promoter, Int. J. Biol. Macromol. 69 (2014) 165–170.
[48] Z. Zheng, Q. Huang, X. Luo, Y. Xiao, W. Cai, H. Ma, Effects and mechanisms of ultrasound-and alkali-assisted enzymolysis on production of water-soluble yeast β-glucan, Bioresource Technol. 273 (2019) 394–403.
[49] S. Hanashima, A. Ikeda, H. Tanaka, Y. Adachi, N. Ohno, T. Takahashi, Y. Yamaguchi, NMR study of short beta (1–3)-glucans provides insights into the structure and interaction with Dectin-1, Glycoconj. J. 31 (3) (2014) 199–207.
[50] F. Shi, J. Shi, Y. Li, Y. Ohya, Mechanochemical phosphorylation and solubilisation of β-D-glucan from Yeast *Saccharomyces cerevisiae* and its biological activities, PLoS ONE 9 (7) (2014) e103494.
[51] T. Rui, Y. Adachi, K.I. Ishibashi, K. Tsubaki, N. Ohno, Binding capacity of a barley beta-D-glucan to the beta-glucan recognition molecule dectin-1, J. Agric. Food Chem. 56 (4) (2008) 1442–1450.
[52] C. Sun, L. Jin, Y. Cai, X. Zheng, T. Yu, (1→3)-β-D-glucan from yeast cell wall: Characteristic and potential application in controlling postharvest disease of pear, Postharvest Biol. Technol. 154 (2019) 105–114.
[53] H. Zheng, S. Cui, B. Sun, B. Zhang, D. Tao, Z. Wang, Y. Zhang, F. Ma, Synergistic effect of discrete ultrasonic and H2O2 on physicochemical properties of chitosan, Carbohyd. Polym. 91 (2022) 119598.